Photophysical Properties of Photoactive Molecules with Conjugated Push−Pull Structures

Ying Gong, Xunmin Guo, Sufan Wang, Hongmei Su, and Andong Xia*

The State Key Laboratory of Molecular Reaction Dynamics, and Beijing National Laboratory for Molecular Sciences (BNLMS), Institute of Chemistry, Chinese Academy of Sciences, Beijing-100080, People's Republic of China

Qingguo He and Fenglian Bai*

Laboratory of Organic Solid, and Beijing National Laboratory for Molecular Sciences (BNLMS), Institute of Chemistry, Chinese Academy of Sciences, Beijing-100080, People's Republic of China

Received: January 22, 2007; In Final Form: February 18, 2007

The photophysical properties of two newly synthesized photoactive compounds with asymmetrical D-π-A structure and symmetrical D-π-A-π-D structure are investigated in different aprotic solvents by steady-state and femtosecond fluorescence depletion measurements. It is found that the asymmetrical DA compound has larger dipole moment change than that of the symmetrical DAD compound upon excitation, where the dipole moments of the two compounds have been estimated using the Lippert−Mataga equation. Furthermore, the steady-state spectral results show that increasing solvent polarity results in small solvatochromic shift in the absorption maxima but a large red shift in the fluorescence maxima for them, indicating that the dipole moment changes mainly reflect the changes of dipole moment in excited-state rather than in ground state. The red-shifted fluorescence band is attributed to an intramolecular charge transfer (ICT) state upon photoexcitation, which could result in a strong interaction with the surrounding solvents to cause the fast solvent reorganization. The resulting ICT states of symmetrical compounds are less polar than the asymmetrical compounds, indicating the different extents of stabilization of solute−solvent interaction in the excited state. Femtosecond fluorescence depletion measurements are further employed to investigate the fast solvation effects and dynamics of the ICT state of these two novel compounds. The femtosecond fluorescence depletion results show that the DA compound has faster solvation time than that of DAD compound, which corresponds to the formation of relaxed ICT state (i.e., a final ICT state with rearranged solvent molecules after solvation) in polar solvents. It is therefore reasonably understood that the ICT compounds with asymmetrical (D-π-A) structure have better performance for those photovoltaic devices, which strongly rely on the nature of the electron push−pull ability, compared to those symmetrical compounds (D-π-A-π-D).

1. Introduction

Organic materials with intramolecular charge-transfer (ICT) properties have motivated the creation of new optoelectronic devices such as electroluminescence devices, solar cells and thin film transistors.[1−5] In these applications, the ICT compounds, which are commonly composed of conjugated electron-donating and electron-accepting groups through π-conjugated linker, play important role in determination of the properties of these devices.[6−8] The introduced ICT in photoactive materials could help to reduce the band gap for red-emission applications.[9−14] To such an aim, many dipolar (D-π-A) and quadrupolar (D-π-A-π-D) or (A-π-D-π-A) compounds are therefore extensively investigated by various photophysical and photochemical means to determine the relationship between the chemical structure and the properties.[5,15−49] Unlike those octupolar and quadrupolar molecules with large two-photon absorption properties, one needs to increase the D−A strength, conjugation length, and high molecular symmetry.[15,17,26,29,43−45] It has been shown that the ICT compounds with asymmetrical structure (D-π-A) have better performance in those photovoltaic devices (such as solar energy cell, organic field-effect transistors and electroluminescence devices), which strongly rely on the nature of the electron push−pull ability compared to those symmetrical compounds (D-π-A-π-D) or (A-π-D-π-A).[9,10,50−52] Such property presents us with an interesting scenario in regards to the different charge-delocalized states between symmetrical and asymmetrical compounds, which may results from the different changes of the dipole moments after excitation.

To comprehensively understand the underlying mechanisms, it is necessary to perform the photophysical studies of the asymmetrical and symmetrical compounds in different solvents, where the solvent effects and dynamics of the ICT state could be important parameters to understand the complex spectral properties with different conjugated structures.

In this paper, we present the results of the photophysical properties and excited-state dynamics of two newly synthesized ICT compounds (DA and DAD) in different solvents by steady-state spectra and femtosecond time-resolved fluorescence depletion measurements. The molecular structures of the two novel ICT compounds (DA and DAD) are shown in Scheme 1, where the di(thiophen-2-yl)benzo[c][1,2,5]thiadiazole was designed as electro-deficient unit and the triphenylamine was designed as electron-rich unit.

The experimental results show that, a larger change in charge distribution for the photoacitive DA compound with asymmetrical D-π-A structure could be induced in the excited-state upon excitation compared to the DAD compound with a symmetrical D-π-A-π-D structure. Such photoinduced intramo-

* Corresponding authors. E-mail: andong@iccas.ac.cn and baifl@iccas.ac.cn.

10.1021/jp0705323 CCC: $37.00
Published on Web 06/09/2007

SCHEME 1: The Molecular Structures for DA (top) and DAD (bottom)

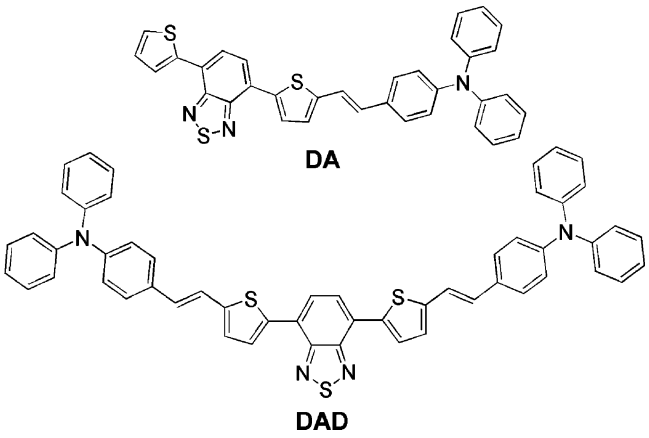

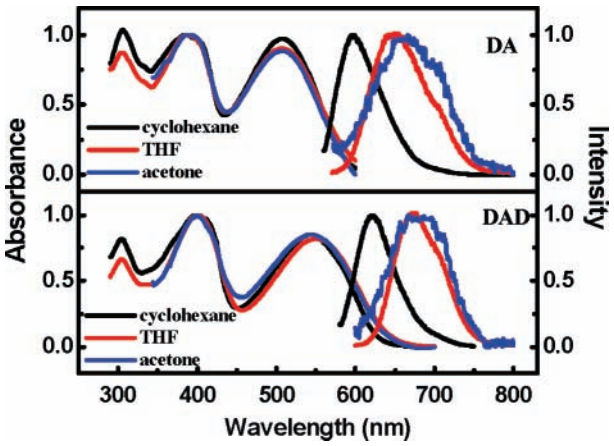

Figure 1. Normalized absorption and fluorescence spectra of DA (top) and DAD (bottom) in different solvents.

lecular charge transfer then results in a strong interaction with the surrounding solvents to cause the solvent reorganization, which is correlated to the large Stokes shift of the fluorescence spectra. The resulting ICT states of symmetrical compounds are less polar than the asymmetrical compounds, indicating the different extents of stabilization of solute−solvent interaction in the excited state. It is of interest to get deeper insight into the underlying photophysical mechanisms of the difference performances in the photovoltaic devices for DA and DAD. The femtosecond time-resolved fluorescence depletion measurements further provide the salvation-dependent information about the very early dynamics of the formation and solvation of the ICT state upon photoexcitation.[53−55] The fast solvation dynamics of these two novel compounds are investigated, suggesting that the solvent has a significant impact on the dynamics of ICT states.

2. Materials and Methods

2.1. Materials. The compounds DA and DAD were synthesized by palladium-catalyzed Heck reaction from N-phenyl-N-(4-vinylphenyl) -benzenamine and 4,7-bis(5-bromothiophen-2-yl) benzo[c][1,2,5] thiadiazole with stoichiometric ratio of 1:1 and 2:1, respectively. Details on the synthesis and characterization will be reported elsewhere.[4] The chemical structures and purities are identified by NMR and MALDI-TOF-MS.

All solvents including cyclohexane, toluene, tetrahydrofuran (THF) and acetonitrile used in this work were of analytical grade, and purchased from the Beijing Chemical Plant with further purification prior to use. The samples were dissolved into different solvents for experiments at a low concentration of 5.0×10^{-5} M in order to avoid aggregation. The resulting solutions were stable, and there was no obvious change checked by absorption spectrum after experiments. All measurements were performed at room temperature.

2.2. Absorption and Fluorescence Measurements. Absorption spectrum was recorded by a UV−vis spectrophotometer (Model U-3010, Shimadzu). Fluorescence spectrum was measured with a fluorescence spectrophotometer (F4500, Hitachi). The fluorescence quantum yields were measured using Rhodamine B ($\phi_f = 0.70$) as standard.[56] All samples were diluted to low concentration, and the optical density was below 0.1 for fluorescence quantum yield measurements in order to minimize self-absorption effect.

2.3. Femtosecond Fluorescence Depletion Measurements. Fluorescence depletion measurements for DA and DAD samples are measured on a homemade femtosecond time-resolved stimulated emission pumping fluorescence depletion (FS TR SEP FD) setup based on the principle of so-called "pump−probe' technology described elsewhere.[53−55] In brief, A CW laser with 532 nm (Verdi-V5, Coherent, USA) pumps a homemade Ti:sapphire laser producing the pulse at 800 nm with duration of about 65 fs at a repetition of 80 MHz. The output power is about 400 mW. This fundamental beam was led into a 1.0 mm thick BBO crystal to produce a second harmonic beam at 400 nm. The second harmonic beam and the residual fundamental beam are split by a dichromic mirror. The ultrafast double-frequency beam at 400 nm ($60 MW/cm^2$) is used for pumping the sample solution to generate the Franck−Condon state; then, the residual ultrafast fundamental pulses at 800 nm ($1.1 GW/cm^2$) with specific polarization (modulated by rotating a zero-level half-wave plate) are introduced as a probe beam to "dump" the population of dye molecules from excited states after a variable delay time. The spontaneous fluorescence emission was perturbed due to compulsive stimulated emission depletion (STED); i.e., the fluorescence was depleted in the presence of dumping pulse. The relative fluorescence intensity depletion at the monitored fluorescence wavelengths (630 nm for DA, and 650 nm for DAD) as a response of delay time was detected via a PMT coupled with a monochromator. A lock-in amplifier is employed to extract the depletion signal correlated to the dumping beam. To avoid the possible thermal effects and photobleaching upon intense femtosecond pulse, sample solution is fluctuated with a high-speed rotor in the sample cell to increase the S/N ratio of detection. In order to get full information about the ultrafast dynamics, we employ here the isotropic (54.7°) femtosecond fluorescence depletion methods, where the polarizations of dumping beams with respect to that of pumping beam are selected by rotating a zero-level half-wave plate to obtain isotropic (54.7°) results. The instrument response function is determined according to the $1 + 1'$ two-photon excited fluorescence method as described before,[53−55] in which the IRF (instrumental response function) up to 125 fs is achieved. All the temporal evolution profiles are fitted by the convolution between the IRF with a muliexponential function according to iterative deconvolution by FluoFit software based on the Levenberg−Marquardt and Simplex algorithms (Version 3.1, PicoQuant, Germany). The fitting quality is judged by weighted residuals and reduced χ^2 values.

3. Results and Discussion

3.1. Steady-State Spectra. Figure 1 shows the absorption and fluorescence spectra of DA and DAD in three different

TABLE 1: Solvent Parameters, Stokes Shifts, and Fluorescence Quantum Yields of DA and DAD

	parameters[a]				Stokes shift (cm^{-1})		Quantum yield	
solvent	ϵ	n	Δf	F^b	DA	DAD	DA	DAD
cyclohexane	2.0	1.424	−0.00330	0	2862.6	2288.4	0.13	0.038
toluene	2.4	1.494	0.0159	0.02	3355.5	2591.9	0.068	0.021
THF	7.6	1.405	0.210	0.44	4238.4	3331.8	0.016	0.0070
MS[c] (1)	9.0	1.402	0.225	0.48	4566.0	3407.2	0.013	0.0058
MS[c] (2)	13.3	1.393	0.253	0.56	4688.2	3596.0	0.0078	0.005
MS[c] (3)	18.9	1.380	0.273	0.62	4823.6	3579.5	0.0042	0.0033
MS[c] (4)	21.6	1.374	0.281	0.65	5048.3	3690.5	0.0019	0.0035
acetone	20.6	1.356	0.285	0.65	4985.6	3868.7	0.0021	0.0030

[a] Parameters are taken from ref 57. [b] F: the reaction field factor[57] [c] MS: mixed solvents of THF and acetonitrile, where MS(1), MS(2), MS(3), and MS(4) represent the mixed solvents of THF/acetonitrile with volume ratio about 9:1, 8:2, 6:4, and 5:5, respectively. The corresponding ϵ_{mix} and n_{mix} are then calculated according to $\epsilon_{mix} = f_a\epsilon_a + f_b\epsilon_b$ and $n_{mix}^2 = f_a n_a^2 + f_b n_b^2$, respectively.[58]

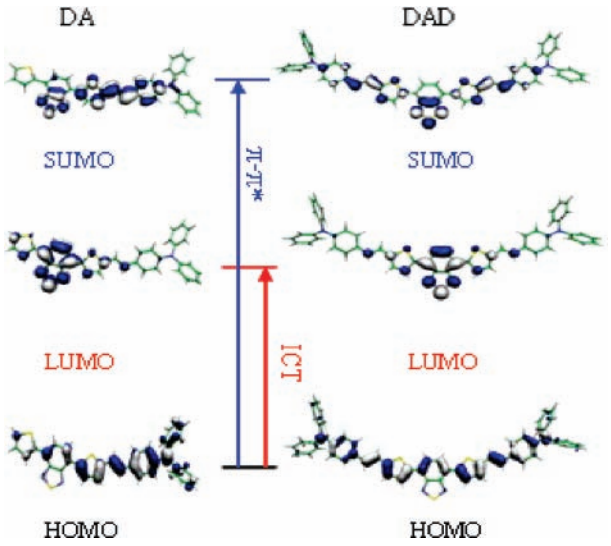

Figure 2. Calculated HOMO, LUMO, and SUMO orbitals of DA and DAD obtained at the B3LYP/6-31g* level.

aprotic solvents. Table 1 lists all the measured steady-state spectral data of DA and DAD in different solvents.

It is found that both DA and DAD molecules show multiple solvent-independent absorption bands with three broad bands peaked around 306 nm, 386 nm and 508 nm for DA and 306, 400, and 550 nm for DAD. The absorption bands around 306 nm for both DA and DAD are mainly attributed to the higher excited-state absorption,[59] which is less sensitive to solvent polarity. The absorption peaks in the wavelength around 386 nm for DA and 400 nm for DAD correspond to the $\pi-\pi^*$ transition, whereas the significant red absorptions for DA at 508 nm and for the DAD at 550 nm might result from the charge-transfer transition within DAD and DA.[3,51,60−63]

To get deeper insight into the nature of ICT state and the absorption bands, the quantum chemical calculations for DA and DAD are performed by density functional theory (DFT) methods as implemented in the Gaussian 03 package.[64] The ground state geometries of DA and DAD have been fully optimized under B3LYP/6-31g* level and the corresponding excited-state single point calculations have been carried out by TD−DFT under the same level. The calculated HOMO (highest occupied molecular orbital), LUMO (lowest unoccupied molecular orbital) and SUMO (second unoccupied molecular orbital) for both compounds DA and DAD, given in Figures 2, clearly show that the optical HOMO−LUMO transition should have a charge-transfer nature, with the electron density shifting mostly from the electron-donating N atom of triphenylamine moieties to the accepting di(thiophen-2-yl) benzo [c][1,2,5]-thiadiazole moieties. Such a localization of the HOMOs and

TABLE 2: Calculated HOMO/LUMO Energies, Energy Gaps, Ground State Dipole Moments of DA and DAD[a]

	HOMO (eV)	LUMO (eV)	SUMO (eV)	$E_g(1)^a$ (eV)	$E_g(2)^b$ (eV)	dipole moment[c] (Debye)
DA	−4.74	−2.58	−1.56	2.16 (2.44)	3.18 (3.26)	2.43 (x)
DAD	−4.57	−2.57	−1.55	2.00 (2.25)	3.02 (3.10)	1.60 (y)

[a] The respective energy gaps observed from absorption spectra are also listed in bracket. [b] $E_g(1)$, energy gap of HOMO−LUMO [c] $E_g(2)$, energy gap of HOMO−SUMO [d] Ground-state dipole moment.

LUMOs on donor−acceptor parts has been reported by previous theoretical research on the other D−A molecules.[65−68] On the other hand, the transition from HOMO to SUMO is mainly assigned as $\pi-\pi^*$ transition, where the bonding to antibonding orbitals of the bridge C=C and the other double bonds of the rings on the main chains of the DA and DAD molecules can be recognized from the calculated orbitals as shown in Figure 2. Table 2 lists the calculated energies of the HOMO, LUMO, and SUMO, as well as energy gaps of the corresponding transitions from HOMO to LUMO and from HOMO to SUMO. The respective energy gaps corresponding to the transitions from HOMO to LUMO and from HOMO to SUMO observed from absorption spectra are also listed in bracket of Table 2 for comparison. It is found that the calculated energy gaps for both DA and DAD are very close to the experimental values obtained from the UV−vis absorption spectra (see Figure 1). The slight diversion between the calculated and experimental values results from the solvation effects for experiments and gas-phase for calculations. In one word, that the HOMO and the SUMO orbitals are delocalized over the whole of the molecules, whereas the LUMO mainly locates on the accepting di(thiophen-2-yl) benzo[c][1,2,5]thiadiazole moieties. Therefore, a significant ICT occurs associated with the HOMO−LUMO transition, which corresponds to the observed absorption around 508 nm for DA and 550 nm for DAD. The HOMO−SUMO absorptions are attributed to the $\pi-\pi^*$ transitions around 386 nm for DA and 400 nm for DAD. The red-shifted absorption and fluorescence compared to those of the DA compound indicates the larger conjugation of DAD compound. Furthermore, as shown in Figure 1, the absorption spectra of both DA and DAD have no major changes with respect to solvent polarity. Similar solvent dependence on optical absorption features is also observed for other donor−acceptor dipolar and octupolar molecules.[69−71]

Unlike the small shift in absorption spectra, a larger solvent-induced shift in emission spectra for both DA and DAD was observed when the solvent polarity was higher. In the fluorescence spectra, the intramolecular charge transfer (ICT) could result in the red-shifted emissions in more polar solvents. This solvatochromism is remarkable; for instance, the shift of DA emission peak is 80 nm from cyclohexane to acetone, and that

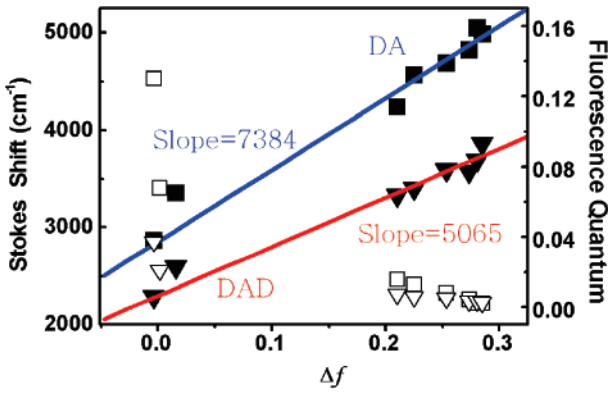

Figure 3. Plot of Stokes shift vs the solvent polarity (Δf) for DA (■) and DAD(▼). Solid lines are the fitted results. Relationship between the quantum yield and Δf of DA (□) and DAD (▽).

of DAD is only 63 nm, indicating the larger dipole moment change occurred in asymmetrical DA compound relative to that of DAD upon excitation. Such properties show that the emitting state of DAD is less polar than that of DA, which result in the different fluorescence quantum yields of DA and DAD. More polar DA in excited-state will lead to larger fluorescence red-shift compared to less polar DAD. The low polar emitting state in the case of the DAD could be due to the charge located on the central part of the symmetrical DAD molecule, and the more polar emitting state of DA is from the localized charge transfer state at one side of the asymmetrical DA molecule, coming by the lower symmetry of the initial excited state. It is found that, in apolar cyclohexane, the fluorescence intensity is more intensive than that in polar solvents, where the fluorescence quantum yield decreases with the increased solvent polarities. Furthermore, a close dual-emission appeared when DA and DAD were dissolved into more polar acetone compared to the single emission peak in apolar cyclohexane.

3.2. Solvation Effects: Solvent Parameters and Spectra. As mentioned above, the absorption spectra of DA and DAD are less dependent on the polarities of solvents, where the extent of the red-shifted fluorescence spectra is strongly dependent on solvent polarities. This indicates that the excited states of DA and DAD could dramatically enter a strongly polar-dependent ICT state from the initial Franck−Condon state in a highly polar medium and lead to large Stokes shifts. The relationship between Stokes shift and solvent polarity was usually given by Lippert−Mataga equation:[72−75]

$$\Delta\nu = \nu_{abs} - \nu_f = \frac{2\Delta f}{hca^3}(\Delta\mu)^2 + \text{const} \quad (1)$$

$$\Delta f = \frac{(\epsilon - 1)}{(2\epsilon + 1)} - \frac{(n^2 - 1)}{(2n^2 + 1)} \quad (2)$$

where $\Delta\nu$ is the Stokes shift, the difference in energy between the absorption and emission maxima; ν_{abs} and ν_f are the wavenumbers of absorption and emission peaks, respectively, h is Planck's constant, c is the speed of light, a is the Onsager cavity radius in which the chromophore resides, and $\Delta\mu = \mu_e - \mu_g$ is the difference between the excited- and ground-state dipole moments as presented by eq 1; Δf is the orientational polarizability of solvent which could deduced from the dielectric constant (ϵ) and the refractive index (n) of the solvent represented by eq 2.

Figure 3 shows the Lippert relationship between the Stokes shifts and solvent polarities. The solvent polarity dependent fluorescence quantum yields of DA and DAD are also displayed in Figure 3 for comparison. We take the Onsager radius a to be 6.79 Å for the DA and 6.81 Å for the DAD, where the Onsager cavity radii (a) are estimated from quantum chemical calculation by using DFT method under B3LYP/6-31g(d) level.

According to the slopes obtained from the fitted results as shown in Figure 3, the difference ($\Delta\mu = \mu_e - \mu_g$) between the ground state and excited-state dipole moments are found to be 14.36 and 11.94 D for DA and DAD, respectively. The obtained values about the excited-state dipole moments of DA and DAD indicate that the symmetrical compounds are less polar in excited-state than the asymmetrical compounds. Such a property with a larger dipole moment change for DA compound indicates that a better performance in the photovoltaic devices could be expected with asymmetric compounds (D-π-A) compared to those symmetrical compounds (D-π-A-π-D).

Furthermore, from Figure 1, it is found that there is no obvious shift of the absorption spectra relative to that of the large red shifts of fluorescence spectra in various solvents indicates that in the excited-state the dipole moment is larger than in the ground state. Therefore, the difference ($\Delta\mu = \mu_e - \mu_g$) could mainly reflects the change of dipole moment in excited state. Therefore, it is reasonably understood that the less polar DAD leads to smaller Stokes shift relative to that of more polar DA from cyclohexane to acetone as mentioned above. This fluorescence sensitivity to solvent is mainly due to the intramolecular charge transfer (ICT) state formation in polar solvent. On one hand, the ICT state could be stabilized by polar solvents, due to stronger interaction between molecules in the excited-state and surrounding solvents. The stabilization of the excited states exhibits the larger red shift of fluorescence spectra in more polar solvents, as shown in Figure 1.

Obviously, a higher polar solvent is much more favorable for solvation-assisted ICT relaxation, and then the nonradiative transition will take a higher portion of the whole deactivation process of excited state, leading to the lower fluorescence quantum yield as shown in Figure 3. On the other hand, an apolar solvent will benefit the fluorescence transition. To determine these properties, femtosecond fluorescence depletion measurements can further provide the solvent-dependent dynamical information about the dynamics of ICT state.

3.3. Fluorescence Depletion Measurements. Femtosecond time-resolved fluorescence depletion technique has been shown a powerful method to determine the fast solvation processes and the formation of the photoinduced ICT state.[53,54,76] As mentioned above, a highly polar ICT state with large dipole moment in DA or DAD compound is produced upon excitation, which could result in the fast solvent reorganization around the excited solute molecule. The more polar dipole moment in the excited-state of asymmetrical compounds will lead to much faster solvation compared to the less polar case of symmetrical compounds, therefore resulting in the faster formation of relaxed ICT state (i.e., a final ICT state with rearranged solvent molecules after solvation). Figure 4 shows the representative femtosecond fluorescence depletion results of DA and DAD in polar THF and acetone. It is found that the dynamic profiles of both DA and DAD can be fitted well with a double-exponential function in THF, and a single-exponential process in more polar acetone. The fitted results are listed in Table 3. In THF, the fast decay less than 1 ps is mainly attributed to vibrational relaxation of the monitored fluorescence states.[53,54] The inertial fast solvation component typical of ~50−100 fs with Gaussian function cannot be distinguished with the used IRF about 125 fs. The slow decay ranging from 1 to 2 ps is manifestation of solvation dynamics related to the formation of ICT state. This

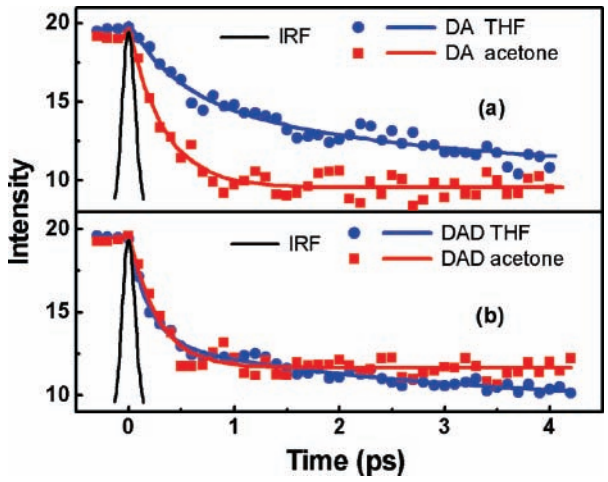

Figure 4. Femtosecond fluorescence depletion signals of DA (a) and DAD (b) in THF and acetone. Dot represents experimental result, and line represents the fitted result. The detection wavelengths are at 630 nm for DA and at 650 nm for DAD. The IRF is also shown at time zero.

TABLE 3: The Fitted Time Constants of Depletion Decays of DA and DAD in Different Solvents[a]

	DA				DAD			
solvent	τ_1 (ps)	A_1	τ_2 (ps)	A_2	τ_1 (ps)	A_1	τ_2 (ps)	A_2
THF	0.445	0.54	2.47	0.46	0.193	0.61	2.83	0.39
acetone	0.332				0.270			
cyclohexane	0.408	0.64	5.33	0.36	0.133	0.80	8.00	0.20

[a] The detection wavelengths are at 630 nm for DA and at 650 nm for DAD.

slow processes about 2.47ps of DA and 2.83ps of DAD are the typical salvation time for THF, which is in agreement with the solvation time of 1.69ps for coumarin 153 in THF.[57] Compared to the amplitude about 39% of DAD, the larger amplitude about 46% for the slow decay of DA in THF indicates the higher polar ICT state is formed in DA upon excitation, and the excited-state relaxation mainly result from the solvation-assisted relaxation of ICT state. In other words, the more polar ICT state will result in the faster solvation time with larger amplitude for DA compound in polar solvent compared to the less polar ICT state of symmetrical DAD compound. The more polar solvent could promote the fast solvation-assisted relaxation of ICT state, where the fluorescence depletion shows a single-exponential decay with time constant about 0.332 ps for DA and 0.27 ps for DAD when DA and DAD are dissolved in more polar acetone. It is easily understood that the solvation could help to lower the energy of excited states and then increase the stimulated emission signals.[77] Acetone has been reported to have faster salvation time down to 0.95 ps compared to THF (salvation time for THF is about 1.69ps).[57] Therefore, the formation of the relaxed ICT states of both DA and DAD in acetone is so fast which are comparable to the fast vibrational relaxation, where the two fast processes (vibrational relaxation and solvation) are strongly competed and indistinguishable. In one word, the resulting ICT state could be stabilized by polar solvents, due to strong interaction between solute in the excited-state and surrounding solvents. Therefore, the fluorescence sensitivity to solvent in polar solvent is mainly due to the intramolecular charge transfer (ICT) state formation.

To further determine how the solvation influences the formation of the relaxed ICT state, an apolar aprotic cyclohexane solvent is chosen for comparison. With the fluorescence depletion measurements, a slow 5.33ps salvation time for DA and 8.0 ps salvation time for DAD, and a fast 0.445 ps vibrational relaxation process for DA and 0.193ps vibrational relaxation process for DAD are clearly identified at the monitored fluorescence state in cyclohexane (see Table 3). It is found that the fast fluorescence depletion decay component has large amplitude up to 64% for DA and 80% for DAD, which mainly results from the vibrational relaxation of the locally excited states because of the weak coupling between solute and solvent. The salvation time is very slow about 5.33ps for DA compound and 8.0ps for DAD compound in apolar cyclohexane, indicating that the solvation relaxation of the ICT state cannot form efficiently because of the lack of stabilization by the apolar solvent. Therefore, the initial relaxation after excitation is mainly dominated by the vibrational relaxation for DA and DAD in apolar cyclohexane.

Finally, it should be mentioned here, the fast decay time of DAD in different solvents is always faster than that of DA in corresponding solvents (See Table 3). The faster decay from DAD compound might result from the excited-state annihilation (probably ICT annihilation)[78] since DAD has two chromophores where DA compound only has one chromophore.

4. Conclusions

In conclusion, we present the results of spectral properties and the dynamics of ICT states of two newly synthesized photoactive compounds with asymmetrical D-π-A structure and symmetrical D-π-A-π-D structure investigated by steady state and femtosecond fluorescence depletion measurements. Steady-state spectral results show that increasing solvent polarity results in small red shift in the absorption maxima but a substantial large red shift in the fluorescence maxima for them. It is found that the asymmetrical DA compound has larger change in charge distribution upon excitation compared to that of symmetrical DAD compound. The dipole moments of the two compounds have been estimated using the Lippert−Mataga equation, which shows that the dipole moment changes mainly reflect the changes of dipole moment in excited-state rather than in ground state, and leading to the formation of ICT state. Such photo-induced intramolecular charge transfer can then result in a strong interaction with the surrounding solvents to cause the solvent reorganization, which is correlated to the large Stokes shift of the fluorescence spectra.

Furthermore, the fast solvation effects and dynamics of the ICT of these two novel compounds are also investigated by femtosecond fluorescence depletion measurements. It is found that the solvent has a significant impact on the dynamics of ICT state. The femtosecond fluorescence depletion results show that the DA compound has faster solvation time than that of DAD compound, which is corresponding to the formation of the relaxed ICT state. This suggests that the photoactive compound with asymmetrical DA structure is expected to have larger changes in charge distribution upon excitation compared to that of the symmetrical DAD structure, where the resulting ICT states of symmetrical compounds are less polar than the asymmetrical compounds. Therefore, it is understood reasonably that the ICT compounds with asymmetrical (D-π-A) structure have better performance in the photovoltaic device applications, which strongly rely on the nature of the electron push−pull ability, compared to those symmetrical compounds (D-π-A-π-D).

Acknowledgment. We sincerely thank Prof. Fan'ao Kong for his constant encouragement and for many valuable discussions. This work was financially supported by NSFC

(No.90306013, No.20473100 and No.20673126), Chinese Academy of Sciences (Y2005018) and State Key Project for Fundamental Research (2003CB716900 and 2006CB806000).

References and Notes

(1) Lai, R. Y.; Fabrizio, E. F.; Lu, L.; Jenekhe, S. A.; Bard, A. J. *J. Am. Chem. Soc.* **2001**, *123*, 9112−9118.
(2) Tang, C. W.; Vanslyke, S. A.; Chen, C. H. *J. Appl. Phys.* **1989**, *65*, 3610−3616.
(3) Sun, X. B.; Liu, Y. Q.; Xu, X. J.; Yang, C. H.; Yu, G.; Chen, S. Y.; Zhao, Z. H.; Qiu, W. F.; Li, Y. F.; Zhu, D. B. *J. Phys. Chem. B* **2005**, *109*, 10786−10792.
(4) He, C.; He, Q. G.; He, Y. Y.; Li, Y. F.; Bai, F. L.; Yang, C. H.; Ding, Y. Q.; Wang, L. X.; Ye, J. P. *Solar Energy Mater. Solar Cells* **2006**, *90*, 1815−1827.
(5) O' Regan, B.; Gratel, M. *Nature* **1991**, *353*, 737−739.
(6) Yu, G.; Gao, J.; Hummelen, J. C.; Wudl, F.; Heeger, A. J. *Science* **1995**, *270*, 1789−1791.
(7) Janssen, R. J.; Sariciftci, N. S.; Hummenlen, J. C. *MRS Bull*. **2005**, *30*, 33−36.
(8) Glasbeek, M.; Zhang, H. *Chem. Rev.* **2004**, *104*, 1929−1954.
(9) Chen, C. H.; Tang, C. W.; Shi, J.; Klubek, K. P. *Thin Solid Films* **2000**, *363*, 327−331.
(10) Li, J.; Liu, D.; Hong, Z.; Tong, S.; Wang, P.; Ma, C.; Lengyel, O.; Lee, C.-S.; Kwong, H.-L.; Lee, S. *Chem. Mater*. **2003**, *15*, 1486−1490.
(11) Thomas, K. R. J.; Lin, J. T.; Velusamy, M.; Tao, Y.-T.; Chuen, C.-H. *Adv. Funct. Mater*. **2004**, *14*, 83−90.
(12) Islam, A.; Cheng, C.-C.; Chi, S.-H.; Lee, S. J.; Hela, P. G.; Chen, I.-C.; Cheng, C.-H. *J. Phys. Chem. B* **2005**, *109*, 5509−5517.
(13) Ho, T.-I.; Elangovan, A.; Hsu, H.-Y.; Yang, S.-W. *J. Phys. Chem. B* **2005**, *109*, 8626−8633.
(14) Kulkarni, A. P.; Wu, P.-T.; Kwon, T. W.; Jenekhe, S. A. *J. Phys. Chem. B* **2005**, *109*, 19584−19594.
(15) He, G. S.; Xu, G. C.; Prasad, P. N.; Reinhardt, B. A.; Bhatt, J. C.; Dillard, A. G. *Opt. Lett.* **1995**, *20*, 435−437.
(16) Kim, O.-K.; Lee, K.-S.; Woo, H. Y.; Kim, K.-S.; He, G. S.; Guang, S. H.; Swiatkiewicz, J.; Prasad, P. N. *Chem. Mater*. **2000**, *12*, 284−286.
(17) Chung, S.-J.; Rumi, M.; Alain, V.; Barlow, S.; Perry, J. W.; Marder, S. R. *J. Am. Chem. Soc*. **2005**, *127*, 10844−10845.
(18) Charlot, M.; Izard, N.; Mongin, O.; Riehl, D.; Blanchard-Desce, M. *Chem. Phys. Lett*. **2006**, *417*, 297−302.
(19) Charlot, M.; Porre's, L.; Entwistle, C. D.; Beeby, A.; Marder, T. B.; Blanchard-Desce, M. *Phys. Chem. Chem. Phys.* **2005**, *7*, 600−606.
(20) Frederiksen, P. K.; Jørgensen, M.; Ogilby, P. R. *J. Am. Chem. Soc.* **2001**, *123*, 1215−1221.
(21) Abbotto, A.; Beverina, L.; Bozio, R.; Facchetti, A.; Ferrante, C.; Pagani, G. A.; Pedron, D.; Signorini, R. *Org. Lett.* **2002**, *4*, 1495−1498.
(22) Kim, O.-K.; Lee, K.-S.; Huang, Z.; Heuer, W. B.; Paik-Sung, C. S. *Opt. Mater*. **2002**, *21*, 559−554.
(23) Iwase, Y.; Kamada, K.; Ohta, K.; Kondo, K. *J. Mater. Chem.* **2003**, *13*, 1575−1581.
(24) Kawamata, J.; Akiba, M.; Tani, T.; Harada, A.; Inagaki, Y. *Chem. Lett.* **2004**, *33*, 448−449.
(25) Strehmel, B.; Amthor, S.; Schelter, J.; Lambert, C. *ChemPhysChem* **2005**, *6*, 893−896.
(26) Albota, M.; Beljonne, J.-L. B.; Ehrlich, J. E.; Fu, J.-Y.; Heikal, A. A.; Hess, S. E.; Kogej, T.; Levin, M. D.; Marder, S. R.; McCord-Maughon, D.; Perry, J. W.; Röckel, H.; Rumi, M.; Subramaniam, G.; Webb, W. W.; Wu, X.-L.; Xu, C. *Science* **1998**, *281*, 1653−1656.
(27) Werts, M. H. V.; Gmouh, S.; Mongin, O.; Pons, T.; Blanchard-Desce, M. *J. Am. Chem. Soc.* **2004**, *126*, 16294−16295.
(28) Pond, S. J. K.; Rumi, M.; Levin, M. D.; Parker, T. C.; Beljonne, D.; Day, M. W.; Brédas, J.-L.; Marder, S. R.; Perry, J. W. *J. Phys. Chem. A* **2002**, *106*, 11470−11480.
(29) Yang, W. J.; Kim, D. Y.; Jeong, M.-Y.; Kim, H. M.; Jeon, S.-J.; Cho, B. R. *Chem. Commun.* **2003**, 2618−2619.
(30) Ventelon, L.; Charier, S.; Moreaux, L.; Mertz, J.; Blanchard-Desce, M. *Angew. Chem., Int. Ed.* **2001**, *40*, 2098−2101.
(31) Rumi, M.; Ehrlich, J. E.; Heikal, A. A.; Perry, J. W.; Barlow, S.; Hu, Z. Y.; McCord-Maughon, D.; Parker, T. C.; Röckel, H.; Thayumanavan, S.; Marder, S. R.; Beljonne, D.; Brédas, J.-L. *J. Am. Chem. Soc.* **2000**, *122*, 9500−9510.
(32) Woo, H. Y.; Liu, B.; Kohler, B.; Korystov, D.; Mikhailovsky, A.; Bazan, G. C. *J. Am. Chem. Soc.* **2005**, *127*, 14721−14729.
(33) Kanis, D. R.; Ratner, M. A.; Marks, T. J. *Chem. Rev*. **1994**, *94*, 195−242.
(34) Marcus, R. A. *Re*V. *Mod. Phys.* **1993**, *65*, 599−610.
(35) Kelley, A. M. *J. Phys. Chem. A* **1999**, *103*, 6891−6903.
(36) Brédas, J.-L.; Cornil, K.; Meyers, F.; Beljonne, D. In *Handbook of Conducting Polymers*; Skotheim, T. A., Elsenbaumer, R. L., Reynolds, J. R., Eds.; Marcel Dekker: New York, 1998; Vol. 1, p 1.
(37) Reichardt, C. *Chem. Rev*. **1994**, *94*, 2319−2358.
(38) Del Zoppo, M.; Castiglioni, C.; Zerbi, G. In *Handbook of Conducting Polymers*; Skotheim, T. A., Elsenbaumer, R. L., Reynolds, J. R., Eds.; Marcel Dekker: New York, 1998; Vol. 1, p 765.
(39) Marder, S. R.; Beratan, D. N.; Cheng, L.-T. *Science* **1991**, *252*, 103−106.
(40) Lin, T. C.; He, G. S.; Prasad, P. N.; Tan, L.-S. *J. Mater. Chem.* **2004**, *14*, 982−991.
(41) Reinhardt, B. A.; Brott, L. L.; Clarson, S. J.; Dillard, A. G.; Bhatt, J. C.; Kannan, R.; Yuan, L.; He, G. S.; Prasad, P. N. *Chem. Mater.* **1998**, *10*, 1863−1874.
(42) Belfield, K. D.; Schafer, K. J.; Mourad, W.; Reinhardt, B. A. *J. Org. Chem.* **2000**, *65*, 4475−4481.
(43) Beverina, L.; Fu, J.; Leclercq, A.; Zojer, E.; Pacher, P.; Barlow, S.; Van Stryland, E. W.; Hagan, D. J.; Brédas, J.-L.; Marder, S. R. *J. Am. Chem. Soc.* **2005**, *127*, 7282−7283.
(44) Ahn, T. K.; Kim, K. S.; Kim, D. Y.; Noh, S. B.; Aratani, N.; Ikeda, C.; Osuka, A.; Kim, D. H. *J. Am. Chem. Soc.* **2006**, *128*, 1700−1704.
(45) Yoon, Z. S.; Kwon, J. H.; Yoon, M. C.; Koh, M. K.; Noh, S. B.; Sessler, J. L.; Lee, J. T.; Seidel, D.; Aguilar, A.; Shimizu, S.; Suzuki, M.; Osuka, A.; Kim, D. H. *J. Am. Chem. Soc.* **2006**, *128*, 14128−14134.
(46) Antonov, L.; Kamada, K.; Ohta, K.; Kamounah, F. S. *Phys. Chem. Chem. Phys.* **2003**, *5*, 1193−1197.
(47) Grabowski, Z. R.; Rotkiewicz, K.; Rettig, W. *Chem. ReV*. **2003**, *103*, 3899−4031.
(48) Rappoport, D.; Furche, F. *J. Am. Chem. Soc.* **2004**, *126*, 1277−1284.
(49) Köhn, A.; Hättig, C. *J. Am. Chem. Soc.* **2004**, *126*, 7399−7410.
(50) Wang, P. F.; Hong, Z. R.; Xie, Z. Y.; Tong, S. W.; Wong, O. Y.; Lee, C.-S.; Wong, N. B.; Huang, L. S.; Lee, S. T. *Chem. Commun.* **2003**, 1664−1665.
(51) Ramakrishna, G.; Bhaskar, A.; Goodson, T., III *J. Phys. Chem. B* **2006**, *110*, 20872−20878.
(52) Fayed, T. A.; Awad, M. K. *Chem. Phys.* **2004**, *303*, 317−326.
(53) Zhong, Q.; Wang, Z.; Sun, Y.; Zhu, Q.; Kong, F. *Chem. Phys. Lett.* **1996**, *248*, 277−282.
(54) He, Y.; Xiong, Y. J.; Wang, Z. H.; Zhu, Q. H.; Kong, F. A. *J. Phys. Chem. A.* **1998**, *102*, 4266−4270.
(55) Guo, X. M.; Xia, A. D. *J. Lumin.* **2007**, *122*−*123*, 532−535.
(56) Derras, J. N.; Crosby, G. A. *J. Chem. Phys.* **1971**, *75*, 991−1024.
(57) Horng, M. L.; Gardecki, J. A.; Papazyan, A.; Maroncelli, M. *J. Phys. Chem*. **1995**, *99*, 17311−17337.
(58) Singh, M. K.; Pal, H.; Bhasikuttan, A. C.; Sapre, A. V. *Photochem. Photobiol*. **1998**, *68*, 32−38.
(59) Li, B.; Tong, R.; Zhu, R. Y.; Meng, F. S.; Tian, H.; Qian, S. X. *J. Phys. Chem. B* **2005**, *109*, 10705−10710.
(60) Sonoda, Y.; Goto, M.; Tsuzuki, S. J.; Tamaoki, N. *J. Phys. Chem. A* **2006**, *110*, 13379−13387.
(61) Kenfack, C. A.; Burger, A.; Mely, Y. *J. Phys. Chem. B* **2006**, *110*, 26327−26336.
(62) Aqad, E.; Lakshmikantham, M. V.; Cava, M. P.; Metzger, R. *J. Org. Chem.* **2005**, *70*, 768−775.
(63) Kulkami, A. P.; Wu, P.-T.; Kwon, T. W.; Jenekhe, S. A. *J. Phys. Chem. B* **2005**, *109*, 19584−19594.
(64) Frisch, M. J. *Gaussian 03*, Revision B.05; Gaussian, Inc.: Pittsburgh, PA, 2003.
(65) Acar, N.; Kurzawa, J.; Fritz, N.; Stockmann, A.; Roman, C.; Schneider, S.; Clark, T. *J. Phys. Chem.* **2003**, *107*, 9530−9541.
(66) Elangovan, A.; Kao, K.-M.; Yang, S.-W.; Chen, Y.-L.; Ho, T.-I.; Su, Y. O. *J. Org. Chem.* **2005**, *70*, 4460−4469.
(67) Marsden, J. A.; Miller, J. J.; Shirtcliff, L. D.; Haley, M. M. *J. Am. Chem. Soc.* **2005**, *127*, 2464−2476.
(68) Ortiz, R. P.; Osuna, R. M.; Delgado, M. C. R.; Casado, J.; Jenekhe, S. A.; Hernandez, V.; Navarrete, L. J. T. *Int. J. Quantum Chem.* **2005**, *104*, 635−644.
(69) Katan, C.; Terenziani, F.; Mongin, O.; Werts, M. H. V.; Porre's, L.; Pons, T.; Mertz, J.; Tretiak, S.; Blanchard-Desce, M. *J. Phys. Chem. A* **2005**, *109*, 3024−3037.
(70) Rogers, J. E.; Slagle, J. E.; McLean, D. G.; Sutherland, R. L.; Sankaran, B.; Kannan, R.; Tan, L.-S.; Fleitz, P. A. *J. Phys. Chem. A* **2004**, *108*, 5514−5520.
(71) Laage, D.; Thompson, W. H.; Blanchard-Desce, M.; Hynes, J. T. *J. Phys. Chem. A* **2003**, *107*, 6032−6046.
(72) Lippert, V. E. *Z. Elektrochem*. **1957**, *61*, 962−975.
(73) Mataga, N.; Kaifu, Y.; Koizumi, M. *Bull. Chem. Soc. Jpn*. **1956**, *29*, 465−471.

(74) Mataga, N. *Bull. Chem. Soc. Jpn.* **1963**, *36*, 654−659.
(75) Lakowicz, J. R. *Principles of Fluorescence Spectroscopy*; Plenum Press: New York, 1983.
(76) Liu, J.-Y.; Fan, W.-H.; Han, K.-L.; Xu, D.-L.; Lou, N.-Q. *J. Phys. Chem. A* **2003**, *107*, 1914−1917.
(77) Martini, I.; Hartland, G. V. *J. Phys. Chem.* **1996**, *100*, 19764−19770.
(78) Fron, E.; Bell, T. D. M.; Vooren, A. V.; Schweitzer, G.; Cornil, J. C.; Beljonne, D.; Toele, P.; Jacob, J.; Müllen, K.; Hofkens, J.; Vander, A. M.; Schryver, F. C. D. *J. Am. Chem. Soc.* **2007**, *129*, 610−619.